8-1-2019

Melanopsin-Containing ipRGCs Are Resistant to Excitotoxic Injury and Maintain Functional Non-Image Forming Behaviors After Insult in a Diurnal Rodent Model

Garrett M. Fogo
Hope College

Dorela D. Shuboni-Mulligan
Michigan State University

Andrew J. Gall
Hope College, gall@hope.edu

Published in: *Neuroscience*, Volume 412, August 1, 2019, pages 105-115.

Melanopsin-containing ipRGCs are resistant to excitotoxic injury and maintain functional non-image forming behaviors after insult in a diurnal rodent model

Garrett M. Fogo[1,2], Dorela D. Shuboni-Mulligan[3], & Andrew J. Gall[1,*]

[1]Department of Psychology and Neuroscience Program
Hope College
Holland, MI, USA

[2] Neuroscience Graduate Program
University of Michigan
Ann Arbor, MI, USA

[3]Department of Radiology
Michigan State University
East Lansing, MI, USA

*Corresponding author:
Andrew J. Gall, Ph.D.
Department of Psychology
Hope College
35 E. 12th Street, Holland, MI, 49423
Phone: 616.395.7729
Fax: 616.395.7163
e-mail: gall@hope.edu

Number of pages: 27
Number of figures: 6
Number of tables: 1
Number of words in manuscript: 6,943
Number of words in Abstract: 248
Number of words in Introduction: 854
Number of words in Discussion: 1,352

Keywords: circadian, retina, retinal ganglion cells, diurnal, behavior, entrainment

Abbreviations: LD: light-dark; ZT: Zeitgeber time; ipRGC: intrinsically photosensitive retinal ganglion cells; IGL: intergeniculate leaflet; LGN: lateral geniculate nucleus; OPT: olivary pretectal nucleus; DD: constant darkness; LL: constant light; PLR: pupillary light reflex; NMDA: *N*-methyl-*D*-aspartic acid

Abstract

Intrinsically photosensitive retinal ganglion cells (ipRGCs) are critical for the light signaling properties of non-image forming vision. Melanopsin-expressing ipRGCs project to retinorecipient brain regions involved in modulating circadian rhythms. Melanopsin has been shown to play an important role in the way animals respond to light, including photoentrainment, masking (i.e., acute behavioral responses to light), and the pupillary light reflex (PLR). Importantly, ipRGCs have been shown to be resistant to various forms of damage, including ocular hypertension, optic nerve crush, and excitotoxicity via *N*-methyl-*D*-aspartic acid (NMDA) administration. Although these cells have been shown to be resistant to various forms of injury, the question still remains whether or not these cells remain functional following injury. Here we tested the hypothesis that ipRGCs would be resistant to excitotoxic damage in a diurnal rodent model, the Nile grass rat (*Arvicanthis niloticus*). In addition, we hypothesized that following insult, grass rats would maintain normal circadian entrainment and masking to light. In order to test these hypotheses, we injected NMDA intraocularly and examined its effect on the survivability of ipRGCs and RGCs, along with testing behavioral and functional consequences. Similar to findings in nocturnal rodents, ipRGCs were spared from significant damage but RGCs were not. Importantly, whereas image-forming vision was significantly impaired, non-image forming vision (i.e, photoentrainment, masking, and PLR) remained functional. The present study aims to shed light on the importance and function of melanopsin with respect to locomotor activity, circadian function, and behavior in response to light in the Nile grass rat.

Introduction

A subset of retinal cells called intrinsically photosensitive retinal ganglion cells (ipRGCs) are responsible for the transduction of non-image forming vision (reviewed in Schmidt & Kofuji, 2008; Hattar et al., 2002). These cells express the photopigment melanopsin (*Opn4*) and project through the retinohypothalamic tract to retinorecipient brain regions important for the regulation of circadian rhythmicity and pupil size (Hannibal et al., 2002; Provencio et al., 1998), including the suprachiasmatic nucleus (SCN; Gooley et al., 2001; Hattar et al., 2002, Mohawk et al., 2012) and olivary pretectal nucleus (OPT; Clarke & Ikeda, 1985), respectively. The intrinsic photosensitive properties of ipRGCs and their projections to the SCN and OPT reveal the central role for melanopsin in the control of light-entrained behaviors in mammals.

In addition to their intrinsic photosensitivity, ipRGCs are uniquely resistant to several traditional models of cellular injury. Melanopsin-containing ipRGCs are resistant to damage using *in vivo* models of ocular hypertension (Li et al., 2006), optic nerve transection (Li et al., 2008; Robinson & Madison, 2004), and excitotoxic agent exposure including administration of *N*-methyl-*D*-aspartic acid (NMDA) (DeParis et al., 2012; Wang et al., 2018). Furthermore, post-mortem studies of patients with mitochondrial optic neuropathies show the relative resistance of ipRGCs in human disease (Cui et al., 2015; La Morgia et al., 2010; Moura et al., 2013). The resilience of ipRGCs suggests that these cells play a critical role in the maintenance of physiological processes and behavioral outputs. While the injury resistance of ipRGCs has been a focus of the field, the functional behavioral consequences of excitotoxic insult has rarely been examined.

The prominent functions of melanopsin-containing ipRGCs are well understood based upon melanopsin (*Opn4*) and ipRGC knockout rodent models with targeted destruction of ipRGCs. Disruptions to the ipRGC system in these models produce abnormalities in circadian responses to light, such as the photoentrainment of locomotor activity (Gompf et al., 2015; Göz et al., 2008; Güler et al., 2008; Hatori et al., 2008; Panda et al., 2002; Ruby et al., 2002), behavioral responses to acute pulses of light, called masking (Mrosovsky & Hattar, 2003; Mure et al., 2007), and the pupillary light reflex (Chen et al., 2011; Hatori et al., 2008; Jones et al., 2013; Lucas et al., 2003). Based on these observations, we identified photoentrainment, masking, and the PLR as targeted measurable behaviors for our study.

The majority of research regarding melanopsin and ipRGCs has been performed using nocturnal animal models, as opposed to diurnal animals. Nocturnal and diurnal organisms differ in the phase of the light/dark cycle where the majority of activity is present. Nocturnal organisms, like most rodents, are active during the dark or lights-off phase, while diurnal organisms, like humans, are active during the lights-on phase of the day. Chronotype differences of nocturnal and diurnal mammals are likely generated by mechanistic differences in the components of non-image forming vision (e.g., in brain areas that respond differently to light). Whereas the SCN is most active during the same phase in nocturnal and diurnal animals (e.g., during the light phase), downstream brain areas such as the intergeniculate leaflet (IGL) play an important role in species-specific responses to light (Gall et al., 2013). Studies using diurnal mammals (e.g., humans and non-human primates) are limited in volume, but indicate similar anatomical positions and functional outputs of melanopsin-containing ipRGCs as those reported in nocturnal rodents

(Gamlin et al., 2007; Hannibal et al., 2004; La Morgia et al., 2016; Ostrin et al., 2018). Nile grass rats (*Arvicanthis Niloticus*) are rodents that are diurnal in both the natural environment and the laboratory, and have been utilized extensively to understand the mechanisms underlying circadian rhythms (Blanchong et al., 1999; Gall et al., 2017; Katona & Smale, 1997; Langel et al., 2014). The projections of ipRGCs to the SCN, IGL, and OPT in Nile grass rats strongly suggest the importance of ipRGCs for circadian modulation and acute responses to light, such as those shown in nocturnal mammals (Langel et al., 2015). Additionally, environmental light intensity affects wheel-running patterns in Nile grass rats, suggesting the influence of melanopsin on behavioral outputs in these rodents (Fogo et al., 2018). Therefore, Nile grass rats are an excellent diurnal rodent model for examining the role of ipRGCs.

The aim of the present study was to examine the relative resistance of melanopsin-containing ipRGCs to excitotoxic cell death and investigate the behavioral outcomes of such injury in a diurnal mammal. We achieved this by administering *N*-methyl-*D*-aspartic acid (NMDA) intraocularly in Nile grass rats in order to ablate traditional retinal ganglion cells (RGCs), while preserving melanopsin-containing ipRGCs. After NMDA administration, behavioral patterns and acute responses to light were examined, in addition to image-forming visual function, the PLR, and anxiety-like behavior. We hypothesized that melanopsin-containing ipRGCs would be resistant to excitotoxic injury and retain the ability to drive targeted light-modulated behaviors. Compared to controls, grass rats expressing a broad and significant loss of RGCs and preservation of ipRGCs displayed normal functional photoentrainment of locomotor activity, masking behavior, and PLRs. These findings suggest that melanopsin-containing ipRGCs are resistant to NMDA-induced

excitotoxicity and maintain their ability to produce light-modulated behavioral patterns and responses after such insult in a diurnal rodent model.

Experimental Procedures

Subjects

A total of 18 adult female Nile grass rats (*Arvicanthis niloticus*) were obtained from the breeding colony at Hope College. Animals were singly housed in Plexiglas cages (34 x 28 x 17 cm) and provided with food (ProLab RMH 2000, PMI Nutrition: Brentwood, MO) and water *ad libitum*. Experimental procedures were conducted in accordance with the National Institutes of Health Guide for the Care and Use of Laboratory Animals (NIH Publication No. 80–23) and were approved by the Institutional Animal Care and Use Committee of Hope College. All efforts were made to minimize the number of animals used in the study.

Intraocular Injections

Animals were anesthetized with isoflurane (2-4% induction, 1-2% maintenance) throughout the duration of injection procedures. Injections were performed by mounting a 10 µL glass syringe (Hamilton, Model #80301, Reno, NV) with a 30G precision glide needle (Becton, Dickinson and Company, Product #305106, Franklin Lakes, NJ) attached to a micromanipulator for greater precision. Sham (n = 6) animals were administered 1.0 µL of 0.1 M phosphate buffered saline (PBS) bilaterally, while NMDA animals (n = 12) were administered 1.0 µL of 100 mM *N*-methyl-*D*-aspartic acid dissolved in 0.1 M PBS (NMDA, Sigma-Aldrich, St. Louis, MO) bilaterally. The solution was administered slowly over the

course of 1 minute and the needle was kept in place for 2 minutes following injection. The needle was then slowly withdrawn from the eye. For post-operative care, ketoprofen (Fort Dodge Animal Health; s.c.; 5 mg/kg body weight) and 1.0 mL of 0.9% sodium chloride (Hispira, Inc., Lake Forest, IL) were administered. After injection procedures, animals were closely monitored and daily health checks were performed.

Locomotor Activity Recordings

Animals were singly housed in a light-controlled room during locomotor activity recording procedures. Cage-top infrared sensors (Starr Life Sciences Corp., Oakmont, PA) were connected to a 24-channel data port (DP-24; Starr Life Sciences Corp., Oakmont, PA), which transmitted to a computer in an adjacent room running Vital View Software for cage locomotor recording (version 1.2, Starr Life Sciences Corp., Oakmont, PA). Activity counts were collected in 1-min bins. Fluorescent lights (Model 7020-2; Lights of America, Walnut, CA) were placed 4 inches above cage-top. Light intensity during the lights-on phase was 1000 lux, and < 5 lux during the lights-off phase. Prior to injections, all animals were maintained on a 12:12 light-dark (LD) cycle with locomotor activity recording for 2 weeks. Post-injection recordings proceeded for at least 3 weeks in 12:12 LD. Directly following 12:12 LD, animals were recorded in constant darkness (DD) for 7 days and constant light (LL) for 7 days. After constant conditions, animals were returned to 12:12 LD for 2 weeks. Following this re-entrainment phase, animals were administered 2 hour masking light pulses during the lights-off phase (1000 lux) at zeitgeber time (ZT)14, ZT18, and ZT22. Animals were given two rest days between light pulses.

During each lighting condition (12:12 LD, DD, LL), total activity counts were quantified using infrared beam breaks. Total activity counts in 12:12 LD were averaged over each condition both pre and post-injection; post-injection activity counts were analyzed during the final week of recording in 12:12 LD. Additionally, total activity counts were summed and averaged during the subjective day (lights-on) and subjective night (lights-off) for each group. A ratio of diurnal activity to total activity was calculated by dividing the number of activity counts during the subjective day by the total number of activity counts in 24 hours. In LD, DD, and LL, the circadian measures of period and alpha were calculated. In LD, activity onset was calculated. Alpha was calculated using the onset of the morning bout to the offset of the evening bout. Onset and offset were identified as described previously (Fogo et al., 2018), by using the Actogram J Program in conjunction with visual inspection of actograms. Masking was assessed by calculating the total activity counts for each subject at ZT14, 18, and 22 during the light pulse and comparing that to the total activity counts the day before in the darkness.

Behavioral Tests

All behavioral tests were conducted during the lights-on phase at the end of the experiment when animals were housed 12:12 LD conditions. For assessment of anxiety-related behaviors, animals were placed in the open field test for 5 min. The apparatus was an open-air box (100 x 100 x 40 cm), and animals were habituated to the experimental room for one hour prior to recording. Behavior was recorded using a USB camera with varifocal lens, 2.8 mm – 12 mm focal length (Item 60528, Stoelting Co., Wood Dale, IL). ANY-maze behavioral tracking software (version 4.99, Stoelting Co., Wood Dale, IL) was

used to track animals and quantify behavior in the open field test. Animals were assessed on the time spent in the center of the open field test; less time spent in the center is a sign of anxiety-like behavior (Kulesskaya & Voikar, 2014).

The Morris Water Maze utilizes visual cues for spatial learning in order to escape water. We performed the Morris Water Maze in order to assess visual acuity. Animals were placed in a pool (150 cm diameter) of room temperature water with animal-safe white paint for opacity. A platform (10 cm x 10 cm) was placed in the pool in a fixed position for all trials and was not visible from the water's surface. Four visual cues were attached to the walls of the pool and remained in fixed positions for all trials. Prior to the first trials, animals were placed on the platform for 1 minute. In the subsequent 4 trials, animals were placed in the pool for each trial and were removed from the pool and dried when the platform was reached. Trial sessions timed out after 1 minute. Animals that did not find the platform were then placed on the platform for 1 minute before removal from the pool. Animals were returned to home cages for 10 minutes between trials. Swimming was recorded and tracked using the same camera and software as described above. The time to find the platform was measured for sham and NMDA subjects in each trial for the assessment of visual acuity.

Pupillary Light Reflex (PLR)

We examined PLR at the end of the experiment while animals were housed in 12:12 LD conditions. To do so, we recorded each grass rat's pupil size in darkness (5 lux of red light) and again in bright light conditions using an LED fiber optic light (1,000 lux; Dolan-Jenner MI-LED-US-B1). The pupils were video recorded using a low-light video camera

(Sony DCR-SR47). The pupil was placed 6 inches from the lens of the camera in all animals. The area of the pupil was calculated using ImageJ when grass rats were in darkness (using infrared from the camera) and following at least 3 seconds of light. The percent change in pupil size was calculated separately for each eye by recording the pupil area in the light, subtracting the pupil area in the darkness, dividing by the area of pupil in the darkness, and multiplying by 100. The percent change in pupil size was averaged across both eyes for each subject.

Perfusion

After at least seven weeks post NMDA injections, grass rats were given intraperitoneal (i.p.) injections of sodium pentobarbital (Ovation Pharmaceutical, Deerfield, IL, USA). All animals were perfused transcardially with 0.01 M phosphate-buffered saline (PBS), pH 7.2, followed by 4% paraformaldehyde (Sigma-Aldrich; PFA) in 0.1 M PB (PLP). Brains and retinas were removed and post-fixed in 4% paraformaldehyde for 4 hours, transferred to a 20% sucrose solution, and stored at 4°C for at least 48 hours. Brains were then stored long-term in a cryoprotectant solution at -20°C, while retinas were immediately processed for immunohistochemistry (see below).

Immunohistochemistry

Retinal tissue was processed using immunohistochemical procedures for double-labeling of Opn4 (melanopsin protein for ipRGC labeling; Do & Yau, 2010) and Brn3a (transcription factor for labeling of traditional RGCs; Nadal-Nicolás et al., 2009). Retinal tissues were rinsed in 0.3% triton-x in 0.01M PBS, then placed in a 1% hydrogen peroxide

solution, followed by normal donkey serum (Jackson ImmunoResearch Laboratories, 017-000-121, West Grove, PA). Retinal tissues were incubated in Opn4 antibody raised in rabbit (1:2,000, PA1-780, Invitrogen, Carlsbad, CA) along with Brn3a antibody raised in mouse (1:500, sc-8429, Santa Cruz Biotechnology, Santa Cruz, CA) for 48 hours. Fluorescently tagged secondary antibodies were used (FITC-conjugated donkey anti-mouse and Cy3-conjugated donkey anti-rabbit; 1:200, Jackson ImmunoResearch Laboratories, West Grove, PA). Glass slides were used to whole mount the retinal tissue and coverslipped with ProLong Gold antifade reagent with DAPI (Life Technologies Corporation, P36931, Eugene, OR).

Cell counting

To assess numbers of Opn4 and Brn3a-immunoreactive cells, observers blind to condition selected a total of 4 regions (250 x 250 μm) of each retina (one from each quadrant) to image using a fluorescent microscope (Zeiss Axioscope equipped with a high resolution digital camera, AxioCam MRC; Göttingen, Germany). ImageJ was used to count the number of Opn4 and Brn3a-positive cells for each region. The number of Opn4 and Brn3a-positive cells for each region were counted bilaterally and divided by two to obtain an average of counts per retina per animal.

Statistical Analysis

One NMDA subject was an outlier, and was removed from all analyses due to activity counts greater than 2 standard deviations from the mean. Therefore, a total of 17 subjects were included in the analyses presented here. A repeated-measures ANOVA was

used to examine differences in total activity counts and percentage of activity during the lights-on with experimental condition (NMDA vs. sham) as the between-subjects factor and time of surgery (pre-surgery vs. post-surgery) as the within subjects factor. A repeated-measures ANOVA was also used to examine differences in total activity counts and light pulses with experimental condition (NMDA vs. sham) as the between-subjects factor and lighting condition as the within-subjects factor. For MWM, a repeated-measures ANOVA was used with experimental condition (NMDA vs. sham) as the between-subjects factor and trial number as the within-subjects factor. All significant interactions from ANOVAs were followed by post hoc tests using independent samples t-tests for comparing experimental condition or paired samples t-tests for comparing time of surgery. For the open field test, PLR, period, alpha (active period), activity onset, and cell counts, independent samples t-tests were performed to examine differences between shams and NMDA treated animals. For all tests, significance was set at $p<.05$. Means are presented with their standard errors.

Results

Histology

Photomicrographs reveal a significant reduction in the number of cells that express Brn3a (RGCs) that survived following injection of NMDA as compared to PBS (Fig 1A). Quantitative analyses using independent-samples t-tests revealed a significant decrease in the number of cells expressing Brn3a in NMDA vs. PBS treated grass rats ($t_{15} = 5.881$, $p < .0001$; Fig 1B), but no significant difference in these groups for melanopsin expressing cells ($t_{15} = 0.974$, $p = .345$; Fig 1C). These results indicate that melanopsin cells are

resistant to damage induced by NMDA injections in grass rats, whereas Brn3a-positive RGCs were significantly damaged.

Activity Patterns

Figure 2 presents actograms of a representative sham and NMDA treated grass rat in 12:12 LD, followed by DD, LL, and back to 12:12 LD. In the final 12:12 LD conditions, grass rats were presented with 2-hour light pulses at night. For total activity counts, a repeated measures ANOVA revealed a significant time x condition interaction ($F_{1,15}$ = 11.396, $p < .005$). Examination of activity patterns revealed no difference for shams pre- vs post-surgery (t_5 = -1.483, p = .198; Figs 3A & 3C), whereas total activity counts were significantly reduced for NMDA treated grass rats pre- vs post-surgery (t_{10} = 3.69, $p < .005$: Figs 3B & 3C). This reduction in activity in NMDA treated grass rats in LD occurred both during the lights-on phase (Pre-surgery: 6456.545 ± 1024.521, Post-surgery: 3286.273 ± 721.969; t_{10} = 4.513, $p < .005$) and lights-off phase (Pre-surgery: 4142.545 ± 626.357, Post-surgery: 2066.636 ± 515.005; t_{10} = 2.489, $p < .05$), suggesting an overall reduction in activity levels in LD that is independent of lighting condition. Importantly, when examining the percentage of activity that was exhibited during the subjective day (the lights-on phase of a 12:12 LD cycle; Fig 3D), a repeated measures ANOVA did not reveal a significant main effect of time ($F_{1,15}$ = 2.565, p = .130) or condition ($F_{1,15}$ = 0.544, p = .472), and also did not reveal a significant interaction between the variables ($F_{1,16}$ = 2.674, p = .123). Therefore, neither shams nor NMDA treated grass rats exhibited a significant difference in diurnality as measured by percentage of activity during the subjective day

between pre- and post-surgery. These results indicate that whereas total activity was significantly reduced in NMDA treated grass rats in LD, diurnality was not.

Period and alpha were calculated in LD, DD, and LL (see Table 1). We found no significant differences between shams and NMDA treated grass rats in any lighting condition (t_{15}s < 1.330, ps > .203). Activity onset time was also not significantly different from shams vs. NMDA treated grass rats in LD (Sham: 4.92 ± 0.20, NMDA: 5.31 ± 0.22; t_{15} = 1.188, p = .253). Altogether, the circadian clock was not affected by NMDA treatment, as indicated by period, alpha, or activity onset time in LD.

Masking

Figure 4 presents the effects of light pulses in grass rats in shams and NMDA treated grass rats. A repeated measures ANOVA revealed a significant main effect of light pulses presented at ZT14 ($F_{1,15}$ = 30.560, p < .0001), ZT18 ($F_{1,15}$ = 26.127, p < .0001), and ZT22 ($F_{1,15}$ = 20.038, p < .0001). However, no significant main effect of condition was obtained for any light pulse at time point ($Fs_{1,15}$ < 0.548, ps > .471), and no light x condition interactions were found ($Fs_{1,15}$ < 3.02, ps > .103). These results suggest that light pulses induced activity in grass rats at all 3 time points, and NMDA treatment did not affect the way grass rats behaved during a light pulse.

PLR

The pupillary light reflex was not affected by RGC loss (Fig 5). Representative photos of the pupillary response to light (Fig 5A) show that the pupil constricts in light as compared to darkness in both shams and NMDA treated grass rats. Quantitative analyses

were performed by examining the average change in pupil area following administration of a brief light pulse (Fig 5B). An independent samples t-test revealed no significant difference between shams and NMDA treated grass rats for the percent change in pupil area (t_{15} = -0.261, p = .798). Therefore, NMDA administration and subsequent RGC loss did not significantly affect the size of the pupil in response to light stimulation.

Anxiety-like behavior & Image-forming vision

Given the observed decrease in locomotor activity after surgery in NMDA- treated grass rats, we hypothesized that the reduction in activity may be due to changes in anxiety-like behavior. Animals were therefore run in the open field test for the assessment of anxiety-like behavior. However, anxiety-like behavior was not affected by NMDA administration and subsequent RGC loss (Fig 6A). An independent samples t-test revealed no significant difference between shams and NMDA treated grass rats for the amount of time spent in the center of the open field apparatus (t_{15} = .467, p = .647; Fig 6A). There was also no significant difference between experimental condition for total activity levels (Sham: 22.654 ± 4.582, NMDA: 21.530 ± 4.463; t_{15} = 0.162, p = .874) or number of entries to the center (Sham: 5.833 ± 2.242, NMDA: 4.909 ± 2.168, t_{15} = 0.273, p = .789) of the open field apparatus.

In the Morris Water Maze, a repeated measures ANOVA revealed a significant trial x condition interaction ($F_{3,45}$ = 5.559, p < .005; Fig 6B). No significant difference between experimental conditions was found for trial 1 (t_{15} = -1.940, p = .071), but a significant increase in time to find platform was found for NMDA treated animals as compared to shams (t_{15} = -4.673, p < .0001). When analyzing results within each condition, shams

exhibited a significant main effect of trial number ($F_{3,15} = 5.045$, $p < .05$), whereas NMDA treated animals did not ($F_{3,30} = 2.376$, $p = .090$), revealing that shams found the platform faster on trial 4 vs. trial 1, whereas NMDA treated animals did not. These results suggest that whereas anxiety was not affected by NMDA administration, image-forming vision was significantly impaired in grass rats.

Discussion

Melanopsin-positive ipRGCs have been shown to respond directly to light (Arroyo et al., 2016), contribute to circadian and masking behavior (Hattar et al., 2003; Mrosovsky & Hattar, 2003), mediate the pupillary light reflex, and are relatively resistant in several experimental models of cellular injury (DeParis et al., 2012; Li et al., 2006; Li et al., 2008; Robinson & Madison, 2004; Wang et al., 2018). In the present study, we demonstrate the resilience of these cells to excitotoxic agent exposure using NMDA and their contribution to non-imaging forming visual functions in a diurnal rodent model. After intraocular NMDA administration in Nile grass rats, we have shown here that melanopsin-containing ipRGCs survive for seven weeks post injection, while traditional RGCs are susceptible to excitotoxic cell death. Furthermore, whereas image-forming vision is significantly impaired following NMDA-induced excitotoxic injury to the retina, light-modulated behaviors are preserved. These findings suggest that melanopsin-containing ipRGCs are resistant to NMDA-induced excitotoxicity and remain functional by continuing to contribute to light-modulated responses in a diurnal rodent model.

Previous observations using nocturnal rodents have shown that ipRGCs are relatively resistant to various models of retinal cell injury (reviewed in Cui et al., 2015).

Importantly, ipRGCs display varying levels of functionality in these models. In mitochondrial dysfunction disorders of the optic nerve, ipRGCs survive and remain functional, in contrast to the loss of traditional RGCs in these diseases (La Morgia et al., 2010; Moura et al., 2013). Interestingly, ipRGCs survive in an experimentally-induced glaucoma rodent model (Li et al., 2006), but human unilateral glaucoma patients display reductions in PLRs, most likely due to a significant reduction in ipRGC function (Nissen et al., 2014). We therefore aimed to evaluate both the survival and functionality of ipRGCs after NMDA administration in a diurnal rodent model. While the mechanisms remain largely unknown, melanopsin-positive ipRGCs are neuroprotected from excitotoxic cellular injury in mice (DeParis et al., 2012; Wang et al., 2018). Here, we extend this observation to a diurnal rodent. Our results show levels of traditional RGC loss and ipRGC survival similar to other studies and we observed these changes after a longer time period than previous studies (DeParis et al., 2012; Wang et al., 2018). The demonstrated inherent injury resistance of these cells, now demonstrated in both diurnal and nocturnal mammals, reinforces their importance for functions with evolutionary significance, such as non-image forming vision and circadian rhythmicity.

Following NMDA administration, Nile grass rats presented a significant impairment in image-forming vision, but no observed abnormalities in non-image forming visual function. Based on performance in the Morris Water Maze, a behavioral task that requires the use of visual cues, NMDA treated grass rats exhibited a significant impairment in the ability to find the platform, suggesting that they exhibited severe visual deficits. This behavioral deficit likely stems from the significant loss of conventional RGCs due to excitotoxic cell death within the retina. However, NMDA treated rats retained the ability to

entrain to light, to respond to acute pulses of light via masking, and to constrict the pupil in response to light via a functional PLR. Results from *Opn4* and ipRGC knockout models in nocturnal rodents suggest that these non-image forming vision-related functions are driven by melanopsin-containing ipRGCs (Göz et al., 2008; Hatori et al., 2008; Panda et al., 2002; Panda et al., 2003; Ruby et al., 2002). Our results suggest that melanopsin-positive ipRGCs remain functional after insult in Nile grass rats and contribute to the retention of normal photoentrainment, masking behavior and PLR.

Although grass rats were capable of entraining and responding to pulses of light (i.e., masking) normally following NMDA-induced excitotoxicity, activity levels were significantly reduced as compared to controls. Importantly, this reduction in activity levels is not directly attributable to anxiety, as damage to image-forming vision did not affect performance in the open field test, similar to results seen in blind mice (Buhot et al., 2001). These results are not surprising given that visual impairments have been shown to result in significant changes in activity levels in several species (Dyer & Weldon, 1975; Hopkins et al., 1987; Kobberling, 1991; Longmuir & Bar-Or, 2000; Marmeleira et al., 2014; O'Hara & Dyer, 1974). Altogether, the decreased home-cage activity levels observed in NMDA treated grass rats were likely not due to anxiety, but rather due to other mediating factors (e.g., glial cell death, RGC cell death, loss of image-forming vision) involved in locomotor activity expression.

The behavioral outcomes observed in the present study, along with anatomical evidence, point to melanopsin cells as primary drivers of light-dependent circadian behaviors and processes. Previous anatomical work in the Nile grass rats has shown that melanopsin-positive retinal cells project largely to retinorecipient brain regions:

suprachiasmatic nucleus (SCN), lateral geniculate nucleus (LGN), intergeniculate leaflet (IGL), and olivary pretectal nucleus (OPT; Langel et al., 2015). All of these areas play important roles in the circadian organization and light-modulating abilities of these diurnal rodents. The SCN is the central circadian clock in mammals and is essential for circadian rhythmicity in Nile grass rats (Gall et al., 2016; Mohawk et al., 2012). The IGL, a subdivision of the lateral geniculate complex, has been shown to play an important role in species-typical masking responses along with contributing to diurnal behavioral patterns in grass rats (Gall et al., 2013). Finally, the OPT is necessary for masking and the PLR in grass rats (Gall et al., 2017). In a recent study, ablation of ipRGCs in rhesus monkeys induced a graded reduction in the PLR in a concentration-dependent manner (Ostrin et al., 2018), providing supporting evidence that these cells play an important role in the PLR in diurnal mammals. Given the sum of anatomical observations and behavioral correlates of melanopsin-containing ipRGCS, we confirmed that circadian rhythms, including diurnality and photoentrainment, masking behavior, and the PLR were not affected by NMDA intraocular administration, most likely because the pathways from ipRGCs to the SCN, IGL, and OPT, respectively, remained intact. Altogether, our results support the overwhelming evidence that these cells must play an important role in the generation and maintenance non-image forming vision functions.

In this study, we aimed to ablate conventional retinal ganglion cells while preserving melanopsin-containing ipRGCs. The post-mortem histological analyses show that NMDA treated grass rats had a significantly lower number of Brn3a-positive cells than shams, and the two groups did not differ significantly in melanopsin-positive cell counts within the retina. These results demonstrate that in a diurnal rodent model, excitotoxic injury using

NMDA does not significantly affect melanopsin-containing ipRGCs, whereas RGCs are significantly reduced. However, the findings of this study are limited due to the survival of a small number of Brn3a-positive cells following NMDA treatment. Importantly, our results are similar to other studies using nocturnal rodents, showing that whereas NMDA does not affect melanopsin cells, Brn3a-positive cells are significantly reduced but not completely ablated (DeParis et al., 2012; Wang et al., 2018). In order to understand the full scope of ipRGC function in Nile grass rats, an ipRGC knockout may need to be utilized. The generation of this model faces many obstacles, as genetically altered lines of this species do not presently exist and current commercially available melanopsin-targeting toxins are not effective in Nile grass rats (A.J. Gall, unpublished data). For continued study, further in-depth image-forming visual functions should be assessed in this NMDA model in order to evaluate the functionality of the few remaining RGCs and the contributions of glial cells (Zhao et al., 2016). Overall, we believe this model of intraocular NMDA administration in Nile grass rats shows promise as a tool for the further study of melanopsin and ipRGCs in a diurnal mammal.

Here our results suggest that melanopsin-containing ipRGCs are resistant to excitotoxic injury *in vivo* and non-image forming vision-dependent behaviors remain functional in a diurnal mammal. This study affirms the previously observed injury resistant abilities of ipRGCs and extends those observations from nocturnal mice to a diurnal mammal. Further, the significant reduction in RGCs, but not ipRGCs, does not disrupt light-dependent behaviors, implying a critical role of melanopsin-containing ipRGCs in the modulation of these behaviors. The findings of this study further our knowledge of ipRGCs and the non-image forming visual system of diurnal mammals.

Acknowledgements

This project was generously supported by the Jacob E. Nyenhuis Grant for Faculty-Student Collaboration by Hope College. Special thanks to startup funds provided by the Division of Social Sciences at Hope College. We also thank W.D. Todd, S. Deats, T.K.H. Groves, and M. Luck for their technical assistance and helpful comments on previous drafts of the manuscript.

References

Arroyo DA, Kirkby LA, Feller MB. (2016). Retinal waves modulate an intraretinal circuit of intrinsically photosensitive retinal ganglion cells. J Neurosci. 36(26): 6892-6905.

Blanchong JA, McElhinny TL, Mahoney MM, Smale L. (1999). Nocturnal and diurnal rhythms in the unstriped Nile rat, Arvicanthis niloticus. J Biol Rhythm. 14(5): 364-377.

Buhot MC, Dubayle D, Malleret G, Javerzat S, Segu L. (2001). Exploration, anxiety, and spatial memory in transgenic anophthalmic mice. Behav Neurosci. 115(2): 455-467.

Chen SK, Badea TC, Hattar S. (2011). Photoentrainment and pupillary light reflex are mediated by distinct populations of ipRGCs. Nature. 476(7358): 92-95.

Clarke, R.J. and Ikeda, H (1985). Luminance and darkness detectors in the olivary and posterior pretectal nuclei and their relationship to the pupillary light reflex in the rat. I. Studies with steady luminance levels. Exp Brain Res. 57: 224-232,

Cui Q, Ren C, Sollars PJ, Pickard GE, So KF. (2015). The injury resistant ability of melanopsin-expressing intrinsically photosensitive retinal ganglion cells. Neuroscience. 284: 845-853.

DeParis SW, Caprara C, Grimm C. (2012). Intrinsically photosensitive retinal ganglion cells are resistant to N-methyl-D-aspartic acid excitotoxicity. Mol Vis. 18: 2814-2827.

Do MT, Yau KW. (2010). Intrinsically photosensitive retinal ganglion cells. Physiol Rev. 90: 1547-1581.

Dyer RS, Weldon DA. (1975). Blindness-induced hyperactivity in several strains of mice. Physiol Behav. 15(5): 439-441.

Fogo GM, Goodwin AM, Khacherian OS, Ledbetter BJ, Gall AJ. (2018). The effects of ambient temperature and lighting intensity on wheel-running behavior in a diurnal rodent, the Nile grass rat (Arvicanthis niloticus). J Comp Psychol. Epub Ahead of Print

Gall AJ, Smale L, Yan L, Nunez AA. (2013). Lesions of the intergeniculate leaflet lead to a reorganization in circadian regulation and a reversal in masking responses to photic stimuli in the Nile grass rat. PLoS ONE 8(6): e67387.

Gall AJ, Shuboni DD, Yan L, Nunez AA, Smale L. (2016). Suprachiasmatic nucleus and subparaventricular zone lesions disrupt circadian rhythmicity but not light-Induced masking behavior in Nile grass rats. J Biol Rhythm. 31(2): 170-181.

Gall AJ, Khacherian OS, Ledbetter B, Deats SP, Luck M, Smale L, Yan L, Nunez AA. (2017). Normal behavioral responses to light and darkness and the pupillary light reflex are dependent upon the olivary pretectal nucleus in the diurnal Nile grass rat. Neuroscience. 355: 225-237.

Gamlin PD, McDougal DH, Pokorny J, Smith VC, Yau KW, Dacey DM. (2007). Human and macaque pupil responses driven by melanopsin-containing retinal ganglion cells. Vision Res. 47(7): 946-954.

Gompf HS, Fuller PM, Hattar S, Saper CB, Lu J. (2015). Impaired circadian photosensitivity in mice lacking glutamate transmission from retinal melanopsin cells. J Biol Rhythm. 30(1): 35-41.

Gooley JJ, Lu J, Chou TC, Scammell TE, Saper CB. (2001). Melanopsin in cells of origin of the retinohypothalamic tract. Nat Neurosci. 4(12): 1165.

Göz D, Studholme K, Lappi DA, Rollag MD, Provencio I, Morin LP. (2008). Targeted destruction of photosensitive retinal ganglion cells with a saporin conjugate alters the effects of light on mouse circadian rhythms. PLoS One. 3(9): e3153.

Güler AD, Ecker JL, Lall GS, Haq S, Altimus CM, Liao HW, Barnard AR, Cahill H et al. (2008). Melanopsin cells are the principal conduits for rod-cone input to non-image-forming vision. Nature. 453(7191): 102-105.

Hannibal J, Hindersson P, Knudsen SM, Georg B, Fahrenkrug J. (2002). The photopigment melanopsin is exclusively present in pituitary adenylate cyclase-activating polypeptide-containing retinal ganglion cells of the retinohypothalamic tract. J Neurosci. 22(1): RC191.

Hannibal J, Hindersson P, Ostergaard J, Georg B, Heegaard S, Larsen PJ, Fahrenkrug J. (2004). Melanopsin is expressed in PACAP-containing retinal ganglion cells of the human retinohypothalamic tract. Invest Ophth Vis Sci. 45(11): 4202-4209.

Hatori M, Le H, Vollmers C, Keding SR, Tanaka N, Buch T, Waisman A, Schmedt C et al. (2008). Inducible ablation of melanopsin-expressing retinal ganglion cells reveals their central role in non-image forming visual responses. PLoS One. 3(6): e2451.

Hattar S, Liao HW, Takao M, Berson DM, Yau KW. (2002). Melanopsin-containing retinal ganglion cells: architecture, projections, and intrinsic photosensitivity. Science. 295(5557): 1065-1070.

Hattar S, Lucas RJ, Mrosovsky N, Thompson S, Douglas RH, Hankins MW, Lem J, Biel M et al. (2003). Melanopsin and rod-cone photoreceptive systems account for all major accessory visual functions in mice. Nature. 424(6944): 76-81.

Hopkins WG, Gaeta H, Thomas AC, Hill PN. (1987). Physical fitness of blind and sighted children. Eur J Appl Physiol O. 56(1): 69-73.

Jones KA, Hatori M, Mure LS, Bramley JR, Artymyshyn R, Hong SP, Marzabadi M, Zhong H et al. (2013). Small-molecule antagonists of melanopsin-mediated phototransduction. Nat Chem Biol. 9(10): 630-635.

Katona C, Smale L. (1997). Wheel-running rhythms in Arvicanthis niloticus. Physiol Behav. 61(3): 365-372.

Kobberling G, Jankowski LW, Leger Luc. (1991). The relationship between aerobic capacity and physical activity in blind and sighted adolescents. J Visual Impair Blin. 85(9): 382-384.

Kulesskaya N, Voikar V. (2014). Assessment of mouse anxiety-like behavior in the light-dark box and open-field arena: role of equipment and procedure. Physiol Behav. 133: 30-38.

La Morgia C, Ross-Cisneros FN, Sadun AA, Hannibal J, Munarini A, Mantovani V, Barboni P, Cantalupo G et al. (2010). Melanopsin retinal ganglion cells are resistant to neurodegeneration in mitochondrial optic neuropathies. Brain. 133(8): 2426-2438.

La Morgia C, Ross-Cisneros FN, Koronyo Y, Hannibal J, Gallassi R, Cantalupo G, Sambati L, Pan BX et al. (2016). Melanopsin retinal ganglion cell loss in Alzheimer disease. Ann Neurol. 79(1): 90-109.

Langel J, Yan L, Nunez AA, Smale L. (2014). Behavioral Masking and cFos Responses to Light in Day- and Night-Active Grass Rats. J Biol Rhythm. 29(3): 192-202.

Langel JL, Smale L, Esquiva G, Hannibal J. (2015). Central melanopsin projections in the diurnal rodent, Arvicanthis niloticus. Front Neuroanat. 9: 93.

Li RS, Chen BY, Tay DK, Chan HH, Pu ML, So KF. (2006). Melanopsin-expressing retinal ganglion cells are more injury-resistant in a chronic ocular hypertension model. Invest Ophth Vis Sci. 47(7): 2951-8.

Li SY, Yau, SY, Chen BY, Tay DK, Lee VW, Pu ML, Chan HH, So KF. (2008). Enhanced survival of melanopsin-expressing retinal ganglion cells after injury is associated with the PI3 K/Akt pathway. Cell Mol Neurobio. 28(8): 1095-1107.

Longmuir P, Bar-Or O. (2000). Factors influencing the physical activity levels of youths with physical and sensory disabilities. Adapt Phys Act Q. 17(1): 40-53.

Lucas RJ, Hattar S, Takao M, Berson DM, Foster RG, Yau KW. (2003). Diminished pupillary light reflex at high irradiances in melanopsin-knockout mice. Science. 299(5604): 245-247.

Marmeleira J, Laranjo L, Marques O, Pereira C. (2014). Physical activity patterns in adults who are blind as assessed by accelerometry. Adapt Phys Act Q. 31(3): 283-296.

Mohawk JA, Green CB, Takahashi JS. (2012). Central and peripheral circadian clocks in mammals. Annu Rev Neurosci. 35: 445-462.

Moura AL, Nagy BV, La Morgia C, Barboni P, Oliveira AG, Salomão SR, Berezovsky A, de Moraes-Filho MN et al. (2013). The pupil light reflex in Leber's hereditary optic neuropathy: evidence for preservation of melanopsin-expressing retinal ganglion cells. Invest Ophth Vis Sci. 54(7): 4471-7.

Mrosovsky N, Hattar S. (2003). Impaired masking responses to light in melanopsin-knockout mice. Chronobiol Int. 20(6): 989-999.

Mure LS, Rieux C, Hattar S, Cooper HM. (2007). Melanopsin-dependent nonvisual responses: evidence for photopigment bistability in vivo. J Biol Rhythm. 22(5): 411-424.

Nadal-Nicolás FM, Jiménez-López M, Sobrado-Calvo P, Nieto-López L, Cánovas-Martínez I, Salinas-Navarro M, Vidal-Sanz M, Agudo M. (2009). Brn3a as a marker of retinal ganglion cells: qualitative and quantitative time course studies in naive and optic nerve-injured retinas. Invest Ophthalmol Vis Sci. 50(8): 3860-3868.

Nissen C, Sander B, Milea D, Kolko M, Herbst K, Hamard P, Lund-Andersen H. (2014). Monochromatic pupillometry in unilateral glaucoma discloses no adaptive changes subserved by the ipRGCs. Front Neurol. 5: 15.

O'Hara MP, Dyer RS. (1974). Locomotor exploratory activity in blind and normal guinea pigs. Physiol Behav. 13(5): 701-702.

Ostrin LA, Strang CE, Chang K, Jnawali A, Hung LF, Arumugam B, Frishman LJ, Smith EL 3rd, Gamlin PD. (2018). Immunotoxin-Induced ablation of the intrinsically photosensitive retinal ganglion cells in Rhesus monkeys. Front Neurol. 9: 1000.

Panda S, Sato TK, Castrucci AM, Rollag MD, DeGrip WJ, Hogenesch JB, Provencio I, Kay SA. (2002). Melanopsin (Opn4) requirement for normal light-induced circadian phase shifting. Science. 298(5601): 2213-2216.

Panda S, Provencio I, Tu DC, Pires SS, Rollag MD, Castrucci AM, Pietcher MT, Sato TK et al. (2003). Melanopsin is required for non-image forming photic responses in blind mice. Science. 301(5632): 525-527.

Provencio I, Jiang G, De Grip WJ, Hayes WP, Rollag MD. (1998). Melanopsin: An opsin in melanophores, brain, and eye. Proc Natl Acad Sci USA. 95(1): 340-345.

Puro DG, Yuan JP, Sucher NJ. (1996). Activation of NMDA receptor-channels in human retinal Müller glial cells inhibits inward-rectifying potassium currents. Vis Neurosci. 13(2): 319-326.

Robinson GA, Madison RD. (2004). Axotomized mouse retinal ganglion cells containing melanopsin show enhanced survival, but not enhanced axon regrowth into a peripheral nerve graft. Vision Res. 44(23): 2667-2674.

Ruby NF, Brennan TJ, Xie X, Cao V, Franken P, Heller HC, O'Hara BF. (2002). Role of melanopsin in circadian responses to light. Science. 298(5601): 2211-2213.

Schmidt TM & Kofuji P. (2008). Novel insights into non-image forming visual processing in the retina. Cellscience. 5(1): 77-83.

Wang S, Gu D, Zhang P, Chen J, Li Y, Xiao H, Zhou G. (2018). Melanopsin-expressing retinal ganglion cells are relatively resistant to excitotoxicity induced by N-methyl-d-aspartate. Neurosci Lett. 662: 368-373.

Zhao X, Pack W, Khan NW, Wong KY. (2016). Prolonged inner retinal photoreception depends on the visual retinoid cycle. Journal of Neuroscience. 36(15): 4209-4219.

Tables

Table 1. Comparisons of period and alpha length across lighting conditions.

	LD		DD		LL	
	Period	Alpha	Period	Alpha	Period	Alpha
Sham	24.04 ± 0.35	14.87 ± 0.42	23.82 ± 0.07	16.89 ± 0.62	24.49 ± 0.09	19.80 ± 0.51
NMDA	24.00 ± 0.05	14.53 ± 0.32	23.79 ± 0.03	16.52 ± 0.25	24.62 ± 0.05	19.32 ± 0.30
	t_{15}=0.477, p=0.640	t_{15}=0.633, p=0.536	t_{15}=0.449, p=0.660	t_{15}=0.657, p=0.521	t_{15}=1.330, p=0.203	t_{15}=0.878, p=0.394

Means ± SEM for period and alpha (in hours) during 12:12 light-dark (LD), constant darkness (DD), and constant light (LL) conditions for shams and NMDA treated grass rats. No significant differences between shams and NMDA treated grass rats were found for period or alpha in any lighting condition (t_{15}s < 1.330, ps > .203).

Figures

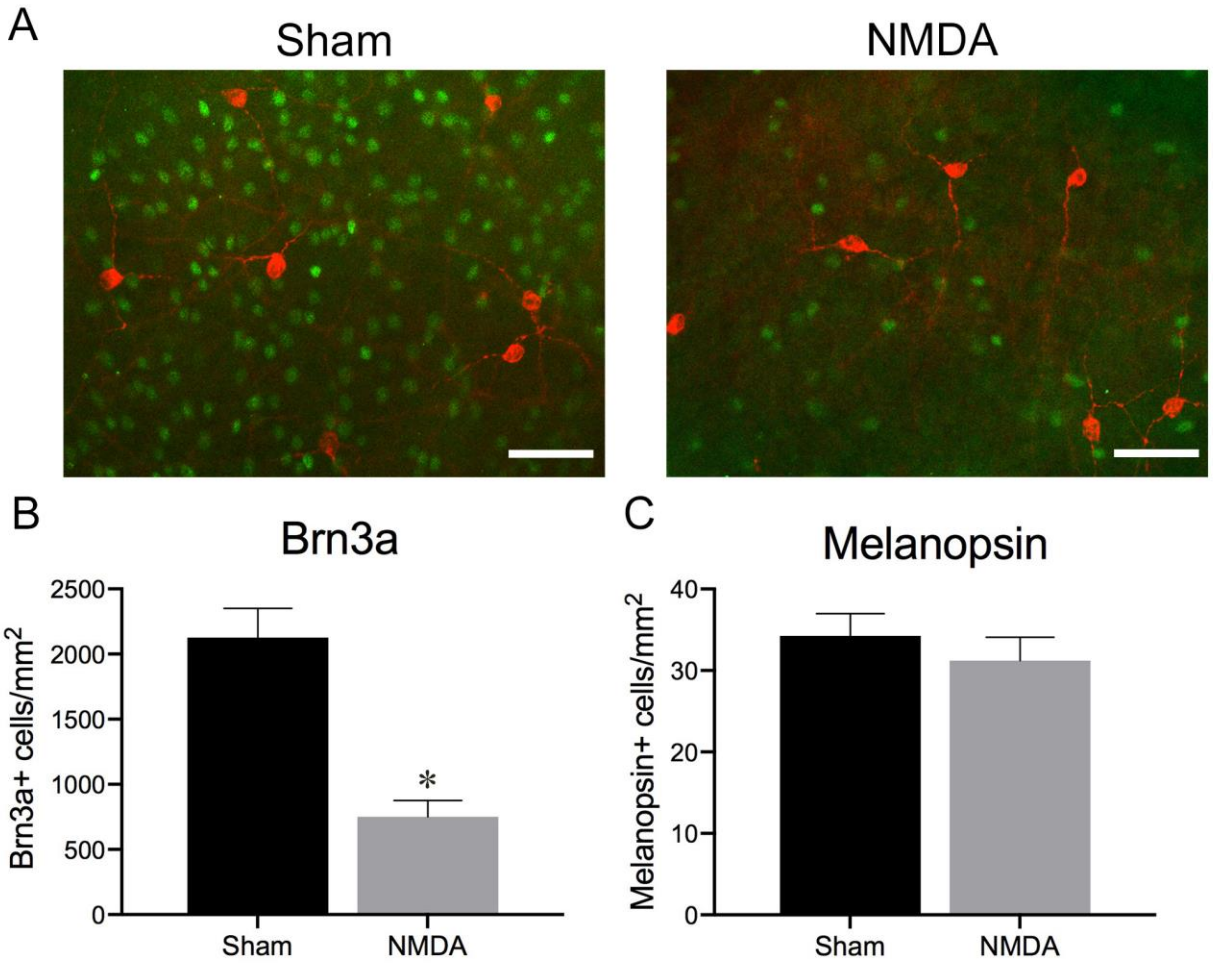

Fig. 1 Identification of intrinsically photosensitive retinal ganglion cells (ipRGCs; melanopsin) and retinal ganglion cells (RGCs; Brn3a) in retinal flat-mounts. (A) Photomicrograph of fluorescent double-labeling of melanopsin (red) and Brn3a (green) in a representative grass rat retina treated with PBS (left) or NMDA (right). Quantitative analyses of Brn3a-positive cells/mm^2 (B) and melanopsin-positive cells/mm^2 (C) in sham (black) and NMDA treated (gray) grass rats. Scale bar represents 50 µm. * indicates $p < .05$, Means ± SEM.

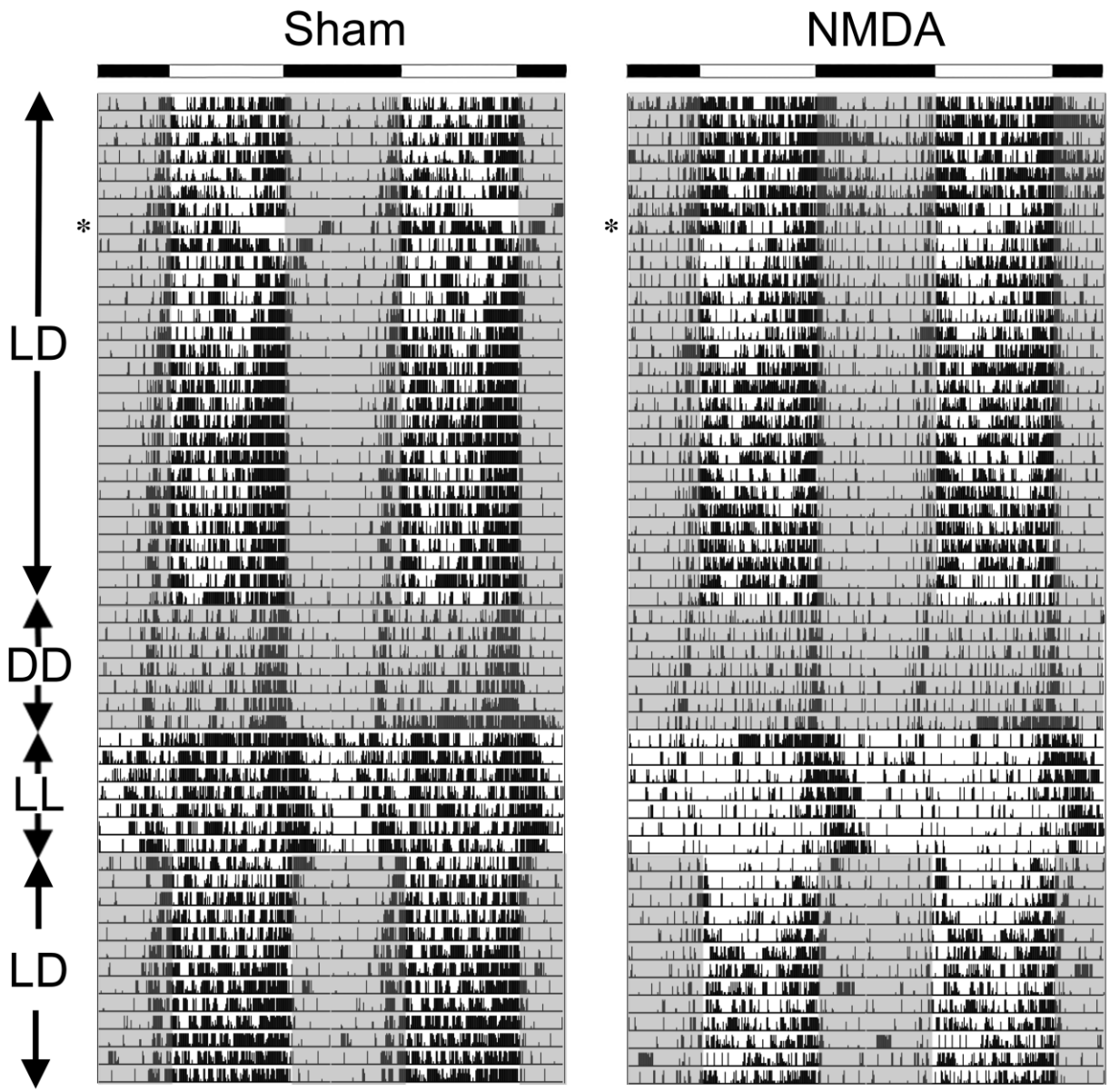

Fig. 2 Representative actograms of a representative sham (left) and NMDA treated grass rat (right). The asterisk indicates day of surgery. Animals were in 12:12 LD, followed by DD, LL, and back to 12:12 LD while presented with 2-hour light pulses at night. Bar at the top indicates lights-on (white) and lights-off (black). Gray shaded regions indicate lights-off.

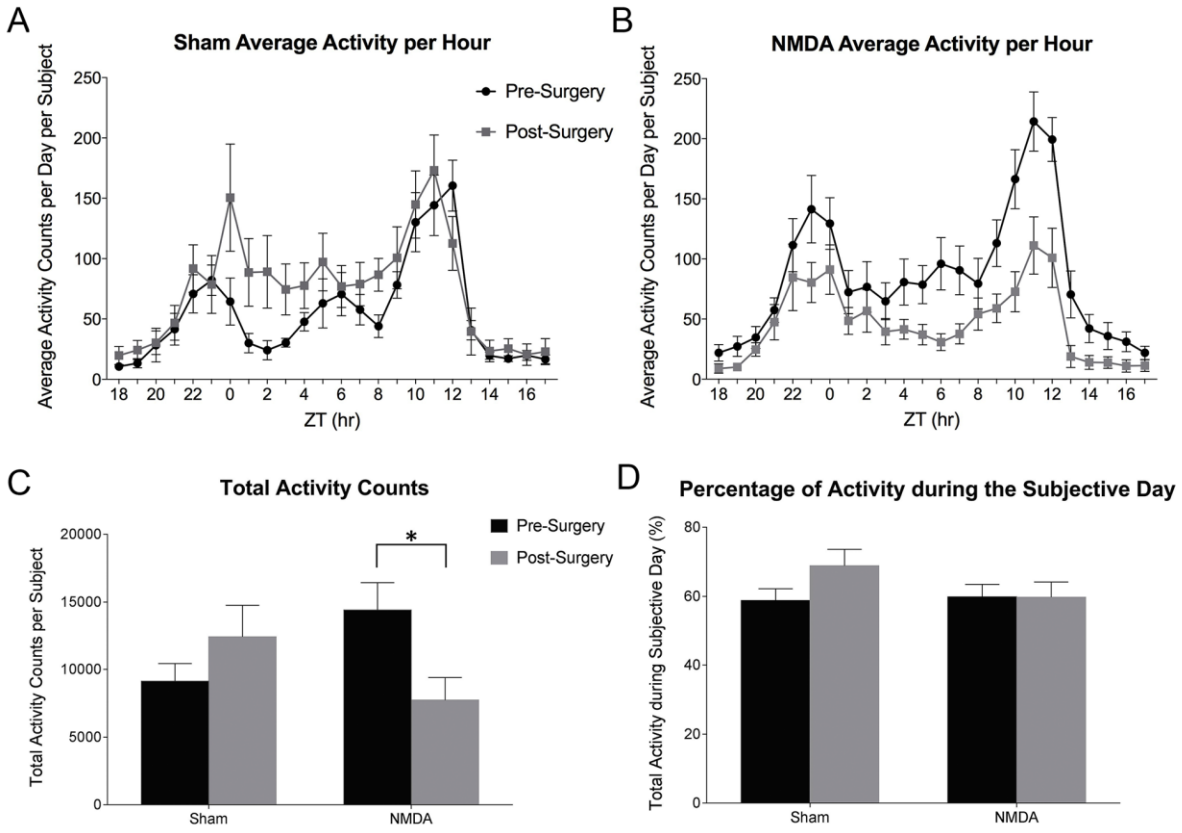

Fig. 3 Activity counts in PBS and NMDA treated grass rats. Average activity per hour per day in shams (A; n=6) and NMDA (B; n=11) treated grass rats. Circles indicate activity pre-surgery, while squares indicate activity post-surgery per Zeitgeber time (ZT). (C) The average sum of all activity counts per subject pre-surgery (black) and post-surgery (gray) in 7 days of 12:12 LD, respectively. (D) Average percentage of total activity counts recorded during the lights-on phase of 12:12 LD pre-surgery (black) and post-surgery (gray). * indicates $p < .05$, Means ± SEM.

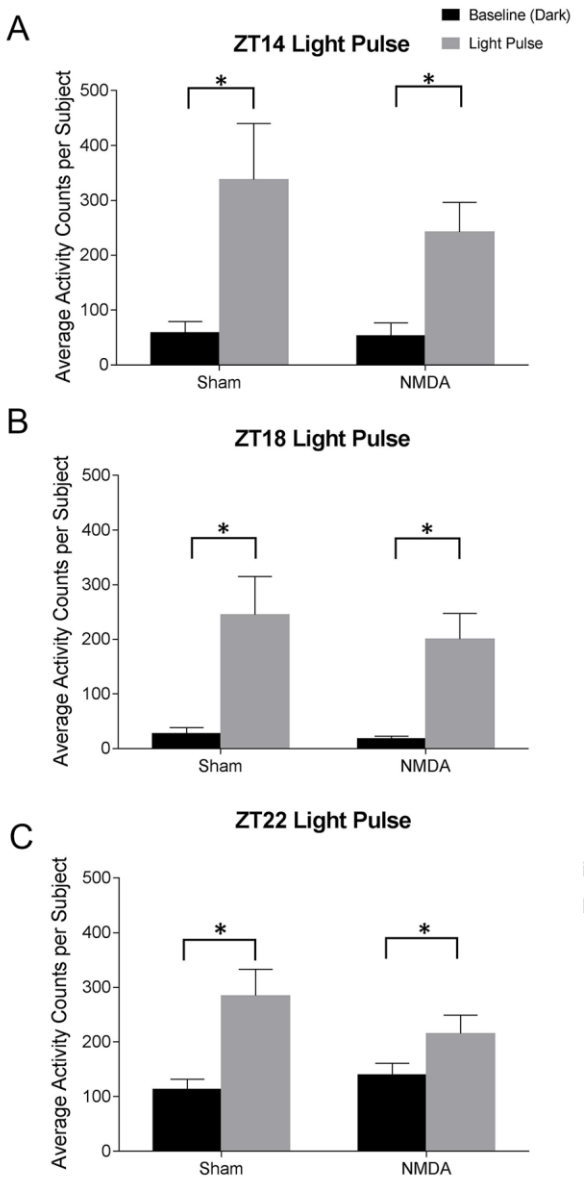

Fig. 4 Average activity counts following a 2-hour acute pulse of light during the dark phase of a 12:12 LD cycle. Activity counts per subject during baseline (activity at the same time point on the day before the light pulse) and during a 2-hour light pulse were presented at ZT14 (A), ZT18 (B), and ZT22 (C). * indicates $p<.05$, Means ± SEM.

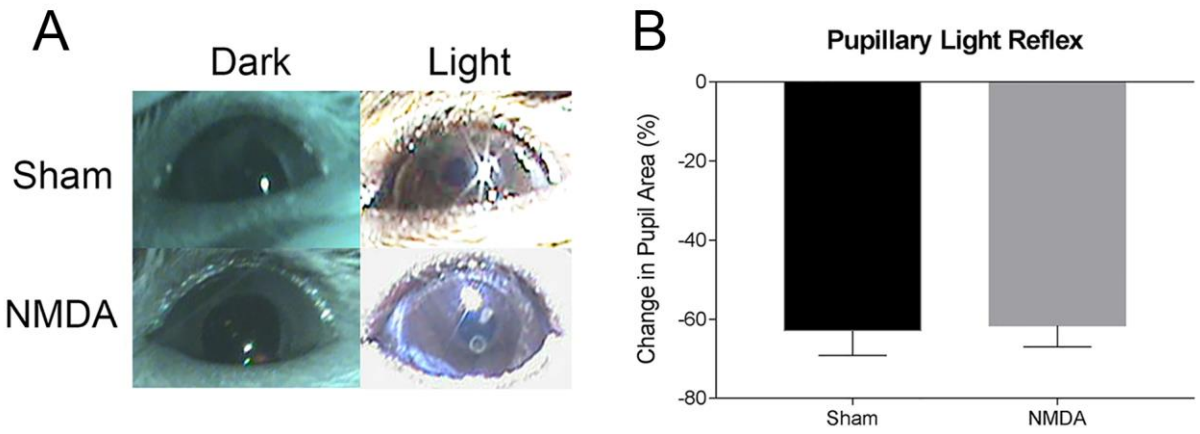

Fig. 5 The pupillary light reflex was not affected by RGC ablation. (A) Representative photos of the pupillary response to light in a sham and NMDA injected animal. Note that the pupillary light reflex was not affected by NMDA treatment. (B) Average percent change in pupil area following administration of a light pulse. Means ± SEM.

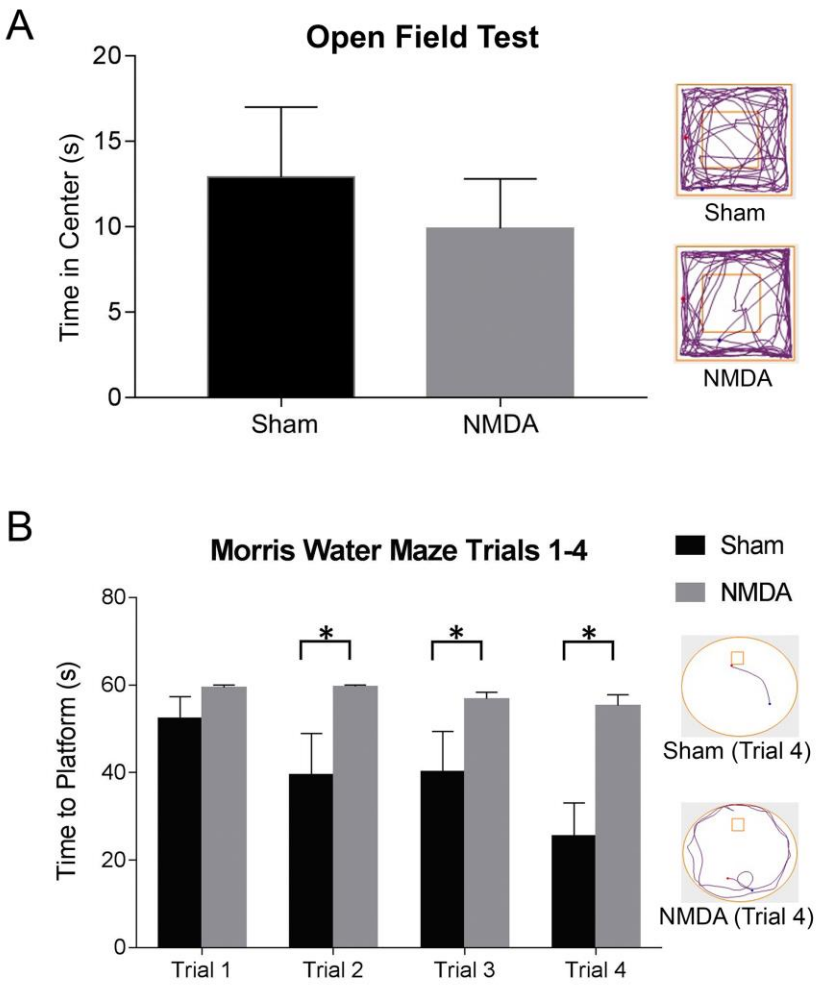

Fig. 6 Anxiety-like behavior was unaffected by RGC ablation, whereas image-forming vision was significantly decreased. (A) Average time in the center zone of the open field test in shams (black) and NMDA (gray) treated grass rats. Representative video tracking of grass rats in the 5-min open field test are presented on the right. (B) Median time to find platform in the Morris Water Maze task for each trial. Open circles indicate individual data points. Representative video tracking of grass rats during trial 4 of the MWM are presented on the right. * indicates $p<.05$. Means ± SEM are presented for open field test in (A); Medians ± median absolute deviations (MADs) are presented for Morris Water Maze in (B).